Available online at www.sciencedirect.com

ScienceDirect

Ceramics International 40 (2014) 399–408

CERAMICS INTERNATIONAL

www.elsevier.com/locate/ceramint

Microstructures and mechanical properties of three-dimensional ceramic filler modified carbon/carbon composites

Yanzhi Cai[a,b,*], Shangwu Fan[a], Xiaowei Yin[a], Litong Zhang[a], Laifei Cheng[a], Yiguang Wang[a]

[a]National Key Laboratory of Thermostructure Composite Materials, Northwestern Polytechnical University, 127#, Youyi Road, Xi'an, Shaanxi 710072, PR China

[b]College of Materials and Mineral Resources, Xi'an University of Architecture and Technology, 13#, Yanta Road, Xi'an, Shaanxi 710055, PR China

Received 23 March 2013; received in revised form 3 June 2013; accepted 3 June 2013
Available online 15 June 2013

Abstract

A three-dimensional needled carbon fiber integrated felt was used as the preform for SiC or B_4C modified carbon/carbon (C/C) composite: C/C–B_4C or C/C–SiC which was prepared through unidirectional pressure slurry infiltration-filtration followed by chemical vapor infiltration. There were four kinds of interface microstructure modes between ceramic filler particles and pyrolytic carbon (PyC) matrix: enwrapping, encircling, embedding and infilling. For C/C–B_4C, enwrapping, encircling and embedding were the main modes. For C/C–SiC, embedding was the main one. The addition of ceramic filler complicated some fiber/matrix interfaces, forming composite interface layers and dual interface layers. There were three kinds of characteristic fiber/matrix interfaces: $(fiber/filler/PyC)_n$/PyC, fiber/(filler/PyC)/PyC, fiber/filler/PyC. The flexure strength of C/C was 98 MPa, whereas those of C/C–B_4C and C/C–SiC were 200 and 140 MPa, respectively. The addition of ceramic filler not only increased the bonding strength of some fiber/matrix interface, but also toughened the PyC matrix.

Keywords: B. Composites; B. Fibers; B. Interfaces; C. Mechanical properties

1. Introduction

For brake materials, not only excellent tribological properties and chemical stability are required, but also good mechanical properties are necessary. A sufficient strength and damage tolerance is of great importance due to the safety sensitiveness of the brake components [1,2]. Low strength and fracture toughness will cause material damage and even catastrophic failure during the braking process. Three-dimensional (3D) needled carbon/carbon (C/C) composites introduce fiber bundles perpendicular to the lamina direction which improves the bonding strength and thermal conductivity between laminates. For C/C brakes, the extremely low friction coefficient in wet and/or corrosive environments represents an obstacle for braking applications [3]; the lower strength of C/C composites is an additional shortcoming having a negative impact on their use.

In order to break the limitations of C/C composites, it is necessary to modify the matrix by introducing some fillers or reinforcements. Park et al. [4,5] prepared C/C composite laminates with $MoSi_2$ filler, the bulk density, graphitization degree and mechanical properties being effectively improved. Gadow et al. [6,7] introduced granular ceramic or ceramic whiskers and slices into multilayer carbon/silicon carbide (C/SiC) composites to reinforce and toughen the matrix. Odeshi et al. [8] prepared two-dimensional (2D) plain weave C fiber reinforced C–SiC dual matrix composites by phenolic resin infiltration-pyrolysis followed by polysilane infiltration-pyrolysis. Their study showed the flexural and visco-elastic properties of the composite were dominated by the strength of the fiber/matrix interface rather than by the strength or modulus of fibers. Li et al. [9] introduced zirconium carbide (ZrC) into 2D C/SiC composites by vacuum infiltration with

*Corresponding author at: National Key Laboratory of Thermostructure Composite Materials, Northwestern Polytechnical University, 127#, Youyi Road, Xi'an, Shaanxi 710072, PR China. Tel./fax: +86 29 82205245.
E-mail address: yzcuxb@aliyun.com (Y. Cai).

0272-8842/$ - see front matter © 2013 Elsevier Ltd and Techna Group S.r.l. All rights reserved.
http://dx.doi.org/10.1016/j.ceramint.2013.06.015

ZrC slurry, higher strength being obtained. Yin et al. [10] improved the mechanical properties of 3D needled C/C composites by TiC slurry infiltration into the porous C/C composite followed by liquid silicon infiltration (LSI) to in-situ synthesize Ti_3SiC_2-SiC matrix in the C matrix. We previously reported on a 3D needled C/SiC composite via graphite modifying SiC matrix, introducing graphite filler having greatly improved the mechanical property [11]. However, as far as we know, few studies on the mechanical properties of 3D needled C/C composites modified by ceramic fillers are reported.

In this study, ceramic filler was introduced to modify C matrix, and the hybrid composites with C matrix reinforced by 3D needled C fibers and ceramic filler particles were prepared. Both SiC and boron carbide (B_4C) have high strength as well as elastic modulus and good chemical inertness. Additionally, B_4C has high specific heat, which can reduce the temperature rise in the braking process. SiC or B_4C filler was introduced into a 3D needled C fiber integrated felt by a new process, unidirectional pressure slurry infiltration-filtration (UPSIF), which was followed by chemical vapor infiltration (CVI) to obtain pyrolytic carbon (PyC) matrix. This new process has an advantage over LSI process in avoiding C fibers damage by molten Si and avoiding the formation of residual Si. The characteristic interfaces in ceramic filler modified C/C composites were revealed. The mechanical behavior between ceramic modified C/C and unmodified C/C composites were compared. The toughening mechanism of ceramic fillers on 3D needled C/C composites was analyzed.

2. Experimental

2.1. Samples preparation

The 3D needled integrated felt with a density of 0.55 g/cm^3 and fiber content of 30 vol% which was described previously in detail [12] was used as the preform. The C fiber was polyacrilonitrile-based C fiber (T 700, 12 K tow, Toray, Japan). The ceramic constituent was introduced into the fiber preform by UPSIF, which was followed by CVI to prepare ceramic filler modified C/C composites.

The fiber preform (ϕ 100 mm × 15 mm) was placed in a unidirectional pressure infiltration-filtration device (Northwestern Polytechnical University, Xi'an, PR China). The bottom side of the preform clung to a millipore membrane. The fiber preform was infiltrated with the slurry containing SiC or B_4C filler powder in water medium under an inert gas pressure-driving from top to bottom. SiC and B_4C filler were 1.0 and 1.5 μm in average particle diameter respectively. The slurry was separated by the millipore membrane at the bottom of the fiber preform. The fiber preform itself is a kind of deep bed filtration medium. Most of the filler particles were retained within the fiber preform and the surface of the millipore membrane. Water and a small quantity of filler particles flowed out. The infiltration pressure and time were 0.6–1.0 MPa and 10–20 min, respectively. The volume fraction of particles in the slurry was 8–12%. All samples were performed only a one-shot infiltration-filtration process, taken out from the device and dried, and then the preform containing SiC or B_4C fillers was obtained.

The CVI process was employed to transform the preform containing the ceramic filler into the hybrid composite with C matrix reinforced by 3D needled C fibers and ceramic fillers. The temperature and time for CVI were 800–1000 °C and 300–400 h, respectively. Propylene was used as a precursor and argon as a carrier as well as diluting gas. The composites prepared by the above method were named as C/C–SiC and C/C–B_4C respectively according to the filler types.

The unmodified C/C composite using the same 3D needled integrated felt as the preform was prepared for comparison. The temperature and time for CVI process to densify the fiber preform were about 800–1000 °C and 400–700 h. Propylene was used as a precursor and argon as a carrier as well as diluting gas.

2.2. Mechanical property testing

The mechanical property of the ceramic modified and unmodified C/C composites was studied using the three-point flexural strength test (SANS CMT 4304, Sans Materials Testing Co., Shenzhen, China). The support span was 30 mm and the cross-head speed 0.5 mm/min. The load direction was perpendicular to the layers of the C felt. Five samples were tested to obtain the average strength. The sample size was 40 × 5 × 3.5 mm^3.

2.3. Microstructure characterization

The open porosities and bulk densities of samples were measured by Archimedes' method. The microstructures and fracture surfaces were examined by scanning electron microscope/energy dispersive X-ray spectroscopy (SEM-EDX, S-4200, Hitachi, Japan). The mass contents of C and SiC in C/C–SiC were determined according to the gravimetric analysis [13]. The content of C was measured by burning it off at 700 °C for 20 h in air, and the SiC-content could be calculated.

3. Results and discussion

3.1. Microstructure characterization

3.1.1. Filler contents and densities

The densities of ceramic filler modified C/C composites were slightly lower than those of the unmodified C/C composite, while the open porosities were higher (Table 1), which was attributed to the shorter densification time. Their densities were greatly reduced compared with those of C/SiC composites (generally higher than 2.00 g/cm^3), which is beneficial for reducing weight of brake materials.

The mass content of SiC filler in C/C–SiC was measured by the gravimetric analysis. The calculation values of volume content v_f and mass content w_f of the ceramic filler in a modified C/C composite were based on the formulas

Table 1
Densities and filler content of C/C composites.

Composites	Density (g/cm^3)	Open porosity (%)	Filler volume content (vol%)	Filler mass content [a] (wt%)
C/C–SiC	1.66	15.8	9.5	18.5/18.0
C/C–B_4C	1.68	16.1	10.4	15.8/–
C/C	1.76	11.1	–	–

[a]Filler mass content was calculation value/test value.

as follows:

$$v_f = 100\% \times (m_2 - m_1)/(\pi r^2 d\rho_f) \quad (1)$$

$$w_f = 100\% \times (v_f \times \rho_f)/\rho_c \quad (2)$$

where ρ_f and ρ_c are the densities of the filler and the corresponding modified C/C composite respectively, m_1 and m_2 are the dry weight of C fiber preform before and after infiltration; r and d are the radius and thickness of the modified C/C composite. From the results listed in Table 1, it is clear the calculated value was close to the test value of SiC content in C/C–SiC. Therefore, it can be extrapolated that it is feasible and effective to obtain the filler contents in the modified C/C composites using the above formulas. The SiC content was close to 20 wt% by only a one-shot infiltration-filtration, indicating this method being of high infiltration efficiency. Therefore, UPSIF has an advantage over the conventional slurry infiltration process [10] in avoiding repeated infiltration cycles.

3.1.2. Filler/matrix interfaces

The interfaces, as the connection zones of C fibers and C matrix or filler particles and C matrix, are the "bridges" of stress transfer. The microstructures and performances of interfaces directly affect the mechanical properties of the composites. Introducing ceramic fillers changed C/C composite into the hybrid composite in which C matrix was reinforced by 3D needled C fibers and ceramic particles. Figs. 1 and 2 show the interface structural modes between filler particles and their surrounding C matrix in ceramic modified C/C composites.

Ceramic fillers were distributed mainly in the fiber sparse areas within the fiber preform. Only a few filler particles entered into the fiber bundles. The areas in Figs. 1 and 2 are both the areas outside of fiber bundles. A prior deposition for PyC in small pore areas within fiber preform, ceramic filler, on the contrary, entered large pores preferentially. The larger pores in short-cut webs and between bundles were divided into smaller pores by ceramic particles which entered in advance, and PyC was then deposited in these smaller pores efficiently.

In C/C–B_4C, the interface microstructure modes between B_4C particles and PyC matrix included four types: enwrapping, encircling, embedding and infilling (Fig. 1), among which enwrapping, encircling and embedding were the main modes. The B_4C/PyC interface mode in Fig. 1(a) was enwrapping, B_4C particles being enwrapped by PyC matrix layer-by-layer into roses in shape. PyC grew layer-by-layer around filler particles and covered filler particles. The well developed graphitized C structure was clear. B_4C particles closed bonded to their surrounding C matrix. One or several B_4C particles were encircled by layered PyC matrix in Fig. 1(b), forming encircling mode interface, and some B_4C particles had dropped out. For encircling mode, PyC grew layer-by-layer around filler particles similar to enwrapping mode but did not developed into a perfect graphite layered structure and not covered filler particles. The bonding between the particle and its surrounding PyC matrix in encircling mode was not as close as that in enwrapping mode. Some B_4C particles were densely distributed in PyC matrix and embedded in it (Fig. 1(c)). PyC did not grow into a layered microstructure due to the restriction of filler particles. PyC deposited in filler particle surfaces, and the interspaces between particles was full of PyC. Additionally, there were a few relatively large B_4C particles filling the voids in PyC matrix to form the infilling mode interface (Fig. 1(d)). For the infilling mode interface, PyC deposited and grew on the surfaces of filler particles but did not fill up the interspaces between filler particles, the filler-PyC bonding being loose.

The C atom in B_4C unit cell is in the active state, and it can be substituted by boron (B) atoms or be detached from the lattice to form the boron-rich compound containing defects. This free C atom detached from the lattice would be used as C crystal nucleus for PyC deposition, so precursor gas would be preferentially deposited around B_4C particles. What is more, as an excellent graphitization catalyst, B_4C could accelerate the graphitization process of PyC. Therefore, the enwrapping and encircling mode B_4C/PyC interfaces were formed. In the areas where B_4C particles were relatively sparse, the amount of C deposited was more and B_4C particles were wrapped up in PyC matrix. In the areas where B_4C particles were relatively dense, the amount of C deposited was less, and B_4C particles were embedded in PyC matrix and evenly dispersed in it.

SiC is different from B_4C in the crystal structure and it is not a graphitization catalyst, so enwrapping and encircling mode SiC/PyC interfaces were not observed in the matrix. The orientation degree of PyC around SiC was not as high as that of PyC around B_4C. Two interface microstructure modes between SiC particles and PyC matrix were observed: embedding and infilling (Fig. 2), among which embedding (Fig. 2(a)) was the main mode. However, larger particles tended to fill in the void in the PyC matrix (Fig. 2(b)). A larger particle had not only the smaller specific surface for deposition, but also a greater probability of a "choking-off" effect. The precursor gas could not smoothly enter into the areas around larger filler

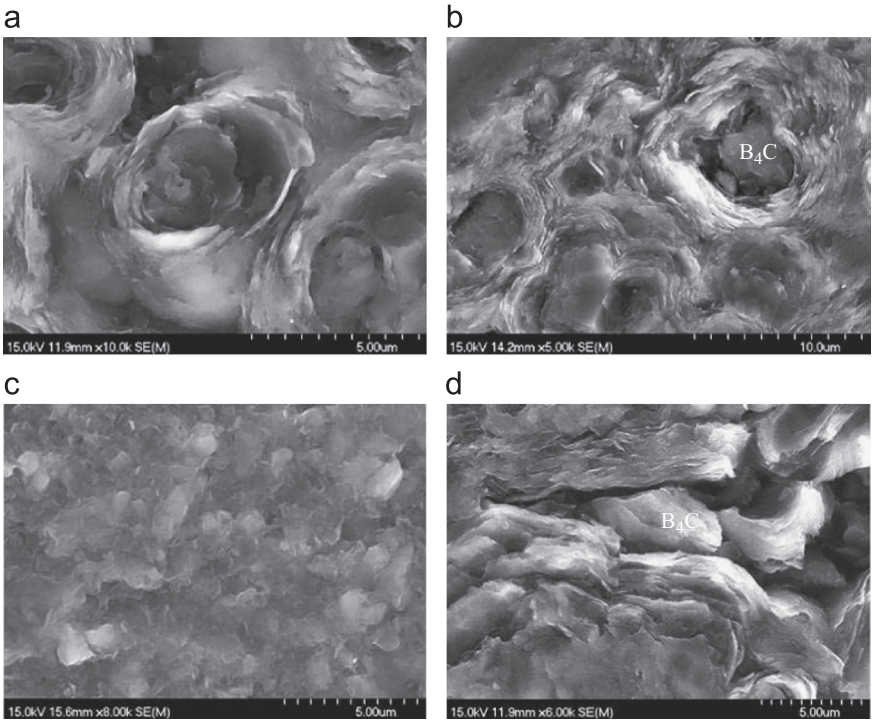

Fig. 1. Interface microstructure modes between B_4C and PyC in C/C–B_4C: (a) enwrapping; (b) encircling; (c) embedding; (d) infilling.

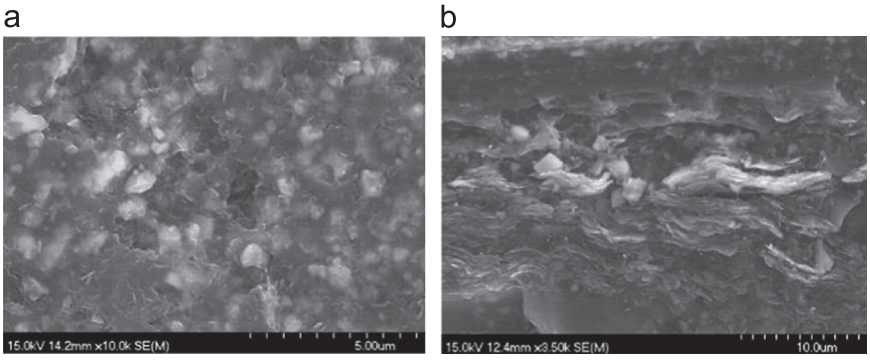

Fig. 2. Interface microstructure modes between SiC and PyC in C/C–SiC: (a) embedding; (b) infilling.

particles, which inclined larger particles towards an interface mode of infilling.

3.1.3. Fiber/matrix interfaces

The fiber/matrix interfaces of ceramic modified and unmodified C/C composites are shown in Fig. 3–5. In unmodified C/C (Fig. 3), the fiber was surrounded by a ring of PyC with layered structure, ring-shaped microcracks existing in most fiber/matrix interfaces. Therefore, fibers had a weak bonding with PyC matrix. In ceramic modified C/C, besides the above weak-bonding fiber/matrix interfaces, the addition of ceramic filler to modify PyC matrix had formed several characteristic fiber/matrix interfaces.

Fig. 4 shows the characteristic fiber/matrix interfaces in C/C–B_4C. In the areas where fibers were sparse, B_4C particles were densely distributed, and C deposited in the surfaces of B_4C particles and fibers, filling the pores between fibers and B_4C particles. B_4C particles randomly distributed around the

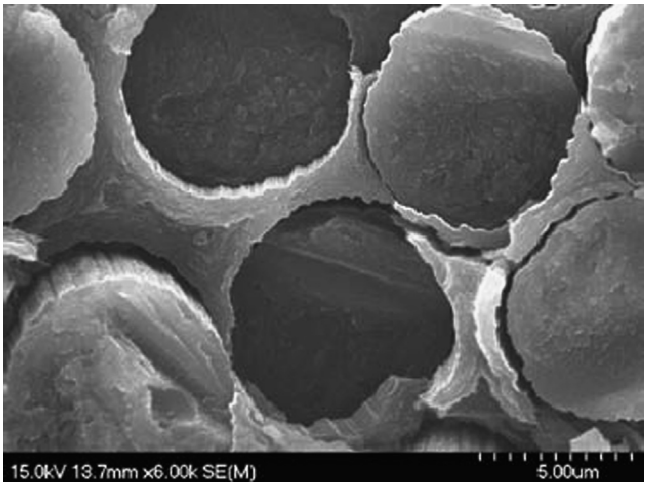

Fig. 3. Fiber/matrix interfaces in unmodified C/C.

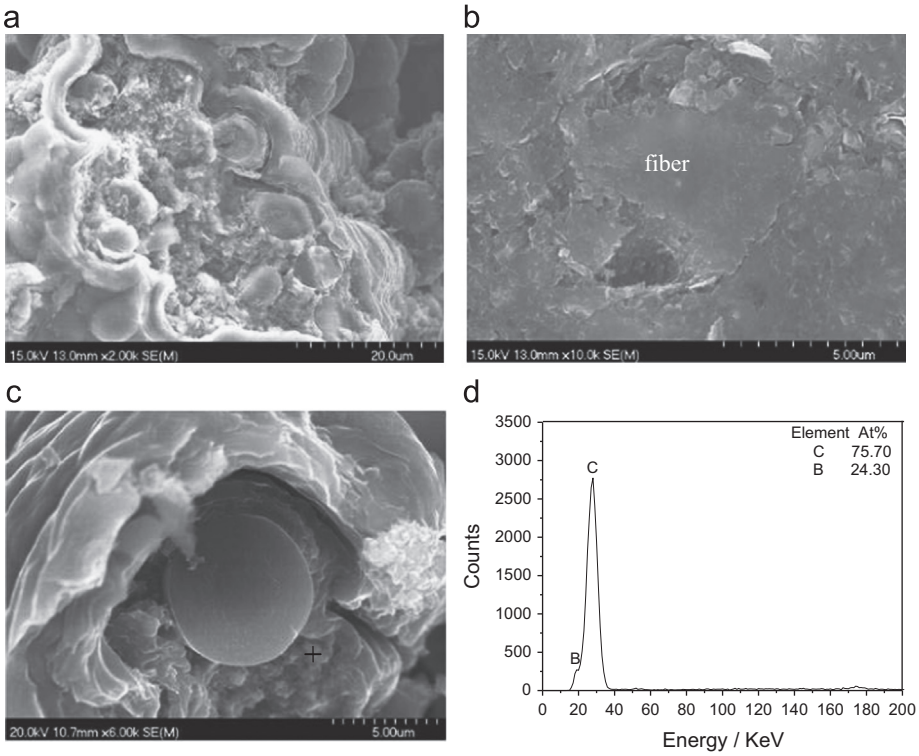

Fig. 4. Fiber/matrix interfaces in C/C–B_4C: (a) (fiber/B_4C/PyC)$_n$/PyC; (b) fiber/B_4C/PyC; (c) fiber/(B_4C/PyC)/PyC; (d) EDX pattern of the site marked in (c).

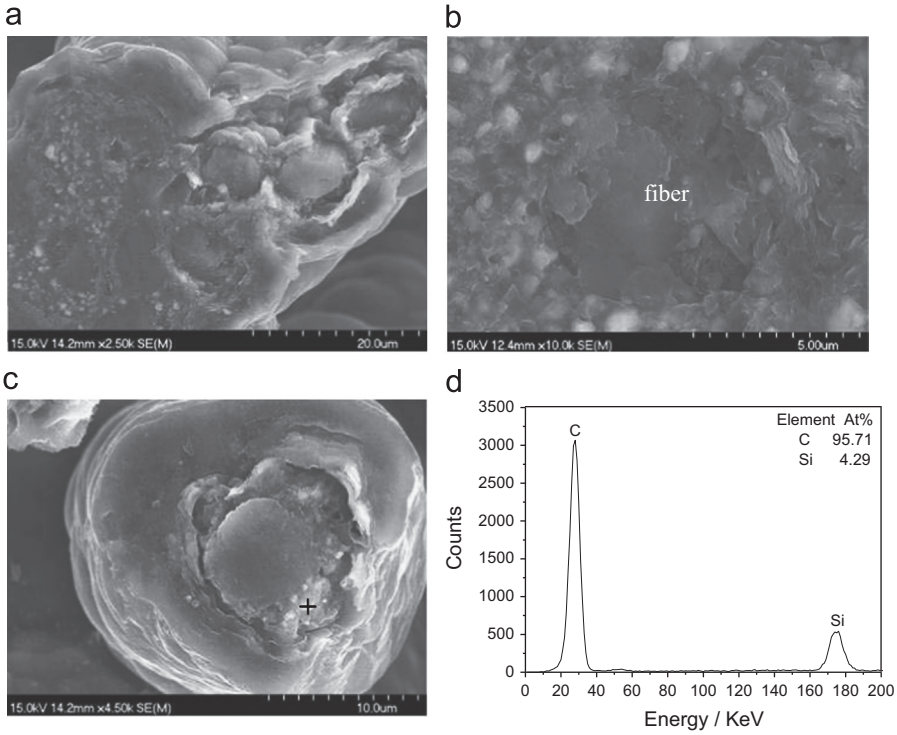

Fig. 5. Fiber/matrix interfaces in C/C–SiC: (a) (fiber/SiC/PyC)$_n$/PyC; (b) fiber/SiC/PyC; (c) fiber/(SiC/PyC)/PyC; (d) EDX pattern of the site marked in (c).

fibers, thus changing the pore shapes and sizes around the fibers, which changed the deposition and growth conditions of PyC around the fibers. Therefore, the fiber/matrix interface was changed. The matrix around the fibers was not PyC single-phase matrix but the composite matrix with ceramic particle dispersion reinforced PyC. These fibers and composite matrix comprised a group which was surrounded by a circle of layered PyC (Fig. 4 (a)). The group was named as fiber–B_4C–PyC cluster and labeled

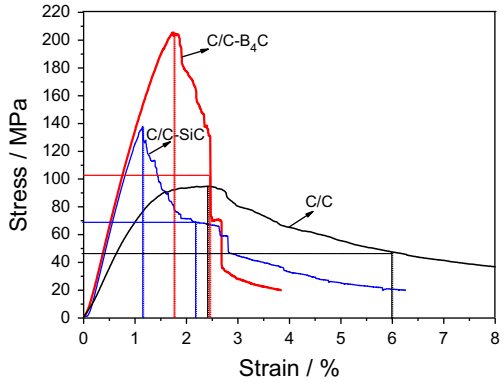

Fig. 6. Flexure stress–strain curves of modified and unmodified C/C composites.

(fiber/B_4C/PyC)$_n$ (the subscript "n" meant more than one fiber) for the convenience of description. The crack existed in the interface between (fiber/B_4C/PyC)$_n$ and PyC, forming a weak bonding between fiber–B_4C–PyC cluster and its surrounding PyC. The fiber/B_4C/PyC interfaces were included in the (fiber/filler/PyC)$_n$/PyC interface, so the latter was called the composite interface.

In some areas inside or outside the fiber–B_4C–PyC cluster, a single fiber was surrounded by PyC and B_4C particles, no ring-shaped microcrack being in the interface, a fiber/B_4C/PyC dual interface layer being formed (Fig. 4(b)). In other areas inside or outside the fiber–B_4C–PyC cluster, B_4C particles as well as PyC around the fiber comprised a group which was surrounded by a ring of PyC with layered structure. A composite interface labeled as fiber/(B_4C/PyC)/PyC was formed (Fig. 4(c)). The mixture of PyC and B_4C particles was a transition layer between the fiber and peripheral PyC. The ring-shaped microcrack existed in the interface between the transition layer and peripheral PyC. The EDS pattern confirmed B_4C particles existed around the single fiber (Fig. 4(d)).

There were several characteristic fiber/matrix interfaces in C/C–SiC similar to those in C/C–B_4C, including (fiber/SiC/PyC)$_n$/PyC, fiber/SiC/PyC, fiber/(SiC/PyC)/PyC, as shown in Fig. 5.

3.2. Mechanical properties

3.2.1. Stress–strain curves

Fig. 6 shows the typical stress–strain curves of ceramic modified and unmodified C/C composites subjected to flexural loading. The curves for C/C–B_4C and C/C–SiC could be divided into three regions: a linear stress–strain behavior before the stress reaching the peak stress; a nonlinear region with increasing strain until the maximum stress level; a step-like region with decreasing stress and increasing strain. The curve shapes for ceramic modified C/C composites exhibit a pseudo-plastic characteristic. The average flexure strength for C/C–B_4C was 200 MPa and for C/C–SiC 140 MPa, while for the unmodified C/C only 98 MPa, so the flexure strength of C/C was only 49% of that of C/C–B_4C and 70% of that of C/C–SiC. The flexure strength of the C/C composite was greatly improved by ceramic modification.

However, after reaching the limit load, the stress of ceramic modified C/C decreased faster than that of the unmodified C/C. The strain values corresponding to the maximum stress values of C/C–B_4C and C/C–SiC were 1.75% and 1.15%, respectively. When the stress value was reduced to half of the maximum value, the corresponding strain value of C/C–B_4C was about 2.5% and that of C/C–SiC about 2.2%. Obviously, the stress value of C/C–B_4C decreased faster than that of C/C–SiC. For the unmodified C/C, the strain value corresponding to the maximum stress value was 2.41% but the one corresponding to half of the maximum stress value was about 6.0%.

The average flexural strength of 3D needled C/SiC composite prepared by CVI combined with LSI in the literature [14] was 165 MPa. The strain value corresponding to the maximum stress value was about 1.2% and corresponding to half of the maximum stress value about 1.7% for this C/SiC composite. The ceramic modified C/C composites were similar to C/SiC composite in the flexural fracture behavior, despite the much lower density and lower ceramic content for the former. The density was 2.10 g/cm^3 for the latter [14] but lower than 1.70 g/cm^3 for the former. The ceramic content was 27 wt% in the latter [14] but lower than 20 wt% in the former. Ceramic filler modified C/C composites had high flexural strength and good fracture toughness, indicating their mechanical properties can meet completely the requirement of aircraft brake materials.

3.2.2. Appearance of facture surface

Fig. 7 shows the appearance of facture surface of unmodified C/C. The unmodified C/C composite had weak fiber–matrix bonding as mentioned above, so the resistance of fiber debonding and sliding was small. From the top view of whole morphology of fracture surface (Fig. 7(a)), the fiber bundles were pulled out and the fibers pulled out were very long. The surfaces of fibers pulled out were clean (Fig. 7(b)). From the amplified photos of single fiber pullout (Fig. 7(c)) and fiber/matrix interfaces after fiber pullout (Fig. 7(d)), either fiber surfaces or fiber/matrix interfaces were clean, only local fiber surface with a thin layer of PyC. In the fiber sparse area, the crack propagated straight through PyC matrix (Fig. 7(e)), and matrix fracture surface was smooth (Fig. 7(f)). These characteristics indicate PyC matrix in the area where fibers are sparse experienced brittle fracture. But the weak fiber/matrix interfaces helped the fibers played their part well in material toughening.

Fig. 8 shows the microscopic fracture profile of C/C–B_4C. The distribution of B_4C particles around fibers (Fig. 4) improved the bonding strength and roughness of fiber/matrix interfaces, so the fiber pullout became more difficulty. Therefore, fibers pulled out were shorter and less, as shown in the top view of whole morphology of fracture surface (Fig. 8(a)). Compared with the unmodified C/C, in addition to some similar interface features after fiber pullout, there were some characteristic interface appearances after fiber pullout.

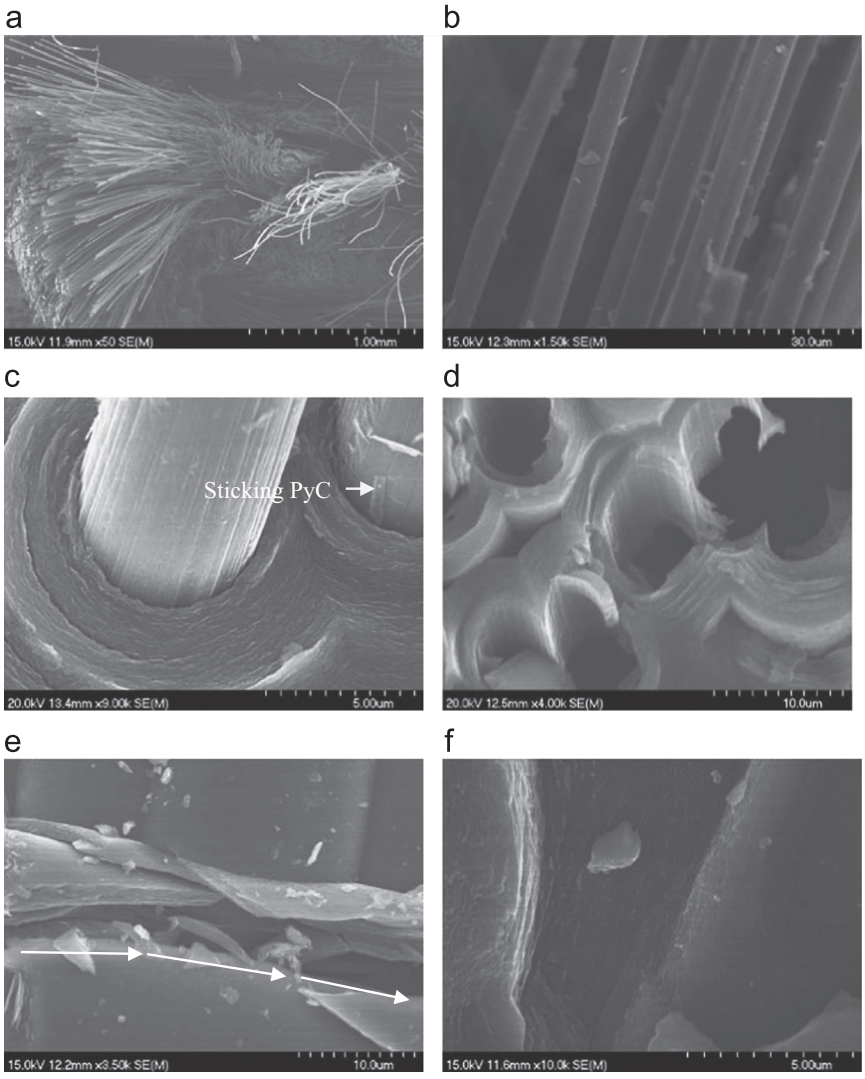

Fig. 7. Fracture profiles of unmodified C/C: (a) fracture surface whole morphology (top view); (b) fiber pullout; (c) amplified photo of fiber pullout; (d) fiber/matrix interfaces after fiber pullout; (e) crack propagation within matrix; (f) magnified matrix fracture surface.

As shown in Fig. 8(b), some matrix materials sticked to the surfaces of fibers pulled out. These characteristics, on one hand, confirmed the improvement of the interface bonding strength between fiber and matrix by B_4C filler, on the other hand, indicated the fiber pullout would consume more fracture energy.

The fiber was surrounded by a ring of matrix materials which was observed in the amplified photo of single fiber pullout (Fig. 8 (c)). In view of the characteristic fiber/matrix interfaces shown in Fig. 4, the matrix materials surrounding the fiber could be identified as PyC and B_4C particles. Further observations on the exposed fiber/matrix interfaces after fiber pullout or fracture, many small pits were left (Fig. 8(d)). The separation of fibers from matrix resulted in B_4C particles pullout from PyC. The addition of ceramic filler complicated the fiber/matrix interface, forming composite interface layers and dual interface layers as mentioned above. B_4C particles meshed with PyC matrix, and C fiber meshed with the composite matrix consisted of PyC and B_4C particles, resulting in a multiple interface debonding process. The fiber–matrix bonding was stronger, the filler particles sticking on the fiber surface was pulled out along with the fiber. Thereby B_4C/PyC debonding was simultaneous with fiber/matrix debonding, resulting in the pits left in fiber/matrix interfaces after fiber pullout.

The crack deflected constantly in matrix during propagation (Fig. 8(e), marked as white arrow). Because ceramic fillers strengthen and toughen PyC matrix, the pullout and fracture of B_4C particles were included in the matrix fracture process. Enwrapping, encircling and embedding were three main B_4C/PyC interface modes in C/C–B_4C, so the bonding strength of B_4C/PyC interface was higher. The intergranular and transgranular fractures were both significant for B_4C particles (Fig. 8 (f)). The matrix fracture surfaces were very rough and rugged (Fig. 8(d)–(f)). Rougher the fracture surface, larger the real fracture surface area was, more the energy was consumed during the fracture process, more difficult to fracture.

As has been demonstrated in Fig. 9, the fracture surface morphology of C/C–SiC was similar to C/C–B_4C, but there were some differences. Because the orientation degree of PyC around SiC was not as high as that of PyC around B_4C, the fiber–matrix bonding in C/C–SiC was not as strong as that in

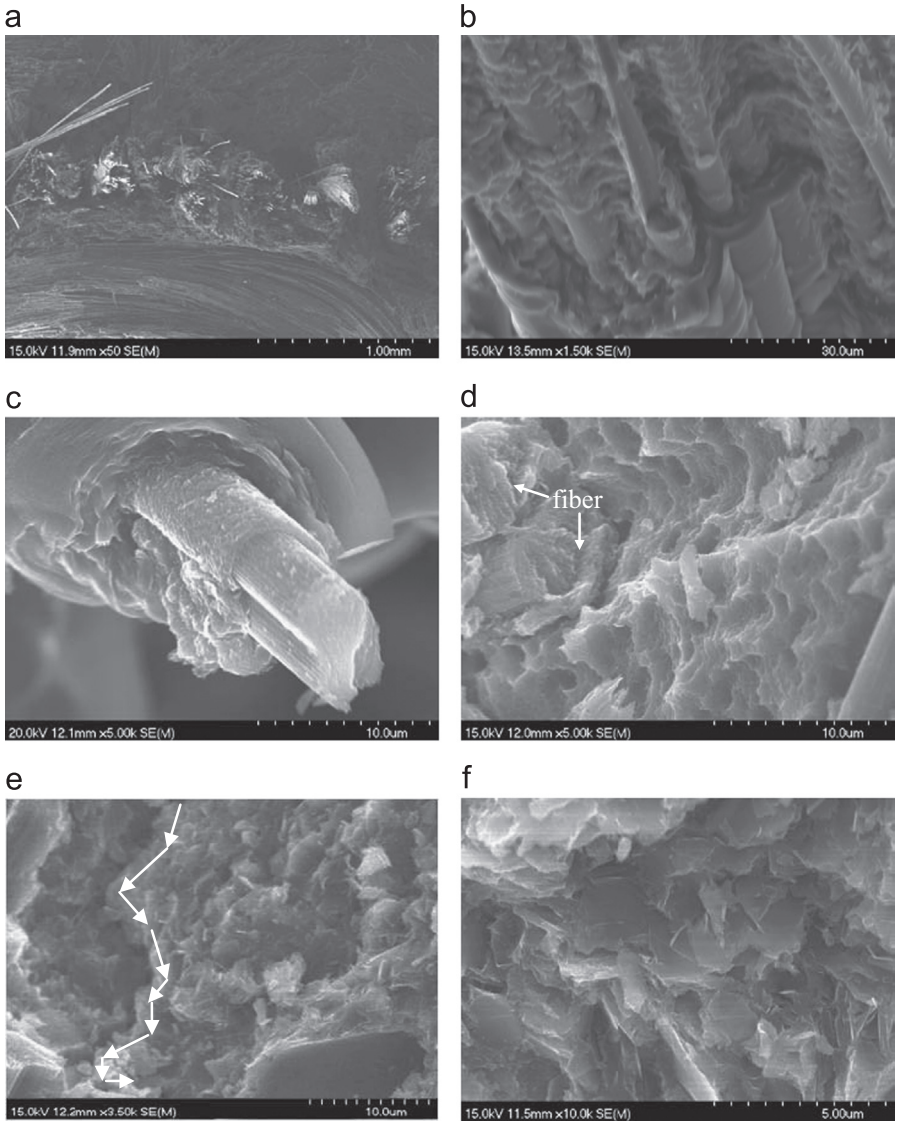

Fig. 8. Fracture profiles of C/C–B_4C: (a) fracture surface whole morphology (top view); (b) fiber pullout; (c) amplified photo of fiber pullout; (d) fiber/matrix interfaces after fiber pullout; (e) crack deflection within matrix; (f) magnified matrix fracture surface.

C/C–B_4C. However, the distribution of SiC particles around fibers increased the roughness of these fiber/matrix interfaces and thus increased the friction between fibers and matrix during fiber pullout process. C/C–SiC was intermediate between unmodified C/C and C/C–B_4C in the length and amount of fiber pullout (Fig. 9(a)). The amount of matrix materials sticking to the surfaces of fibers pulled out in C/C–SiC was less than that in C/C–B_4C (Fig. 9(b)), showing these fiber/matrix interfaces in C/C–SiC was weaker than those in C/C–B_4C. The surfaces of a few single fibers were surrounded by matrix materials after pullout (Fig. 9(c)). In view of the characteristic fiber/matrix interfaces shown in Fig. 5, the materials surrounding fibers could be identified as PyC and SiC particles.

From the exposed fiber/matrix interfaces after fiber pullout (Fig. 9(d)), the rough interfaces were visible, but most SiC particles remained in the PyC matrix rather than pullout along with the fibers. This indicates the fiber–matrix bonding in C/C–SiC was weaker than that in C/C–B_4C. The crack deflected constantly in matrix during propagation (Fig. 9(e), marked as white arrow). The fracture mode for SiC particles was mainly intergranular fracture (Fig. 9(f)). The pits and outcrops which resulted from SiC particle pullout were observed in the fractured surface. This shows the filler/matrix interface in C/C–SiC was also weaker than that in C/C–B_4C. Similar to C/C–B_4C but different from C/C, the matrix fracture surface was rough (Fig. 9(d)–(f)), indicating the fracture of the composite matrix was of difficulty.

4. Conclusions

(1) 3D needled ceramic modified C/C composites: C/C–B_4C and C/C–SiC were prepared using UPSIF followed by CVI. The contents of SiC and B_4C introduced by a one-shot infiltration were about 18 wt% and 16 wt% respectively.
(2) There were four kinds of interface microstructure modes between ceramic filler particles and PyC matrix: enwrapping, encircling, embedding and infilling. For C/C–B_4C,

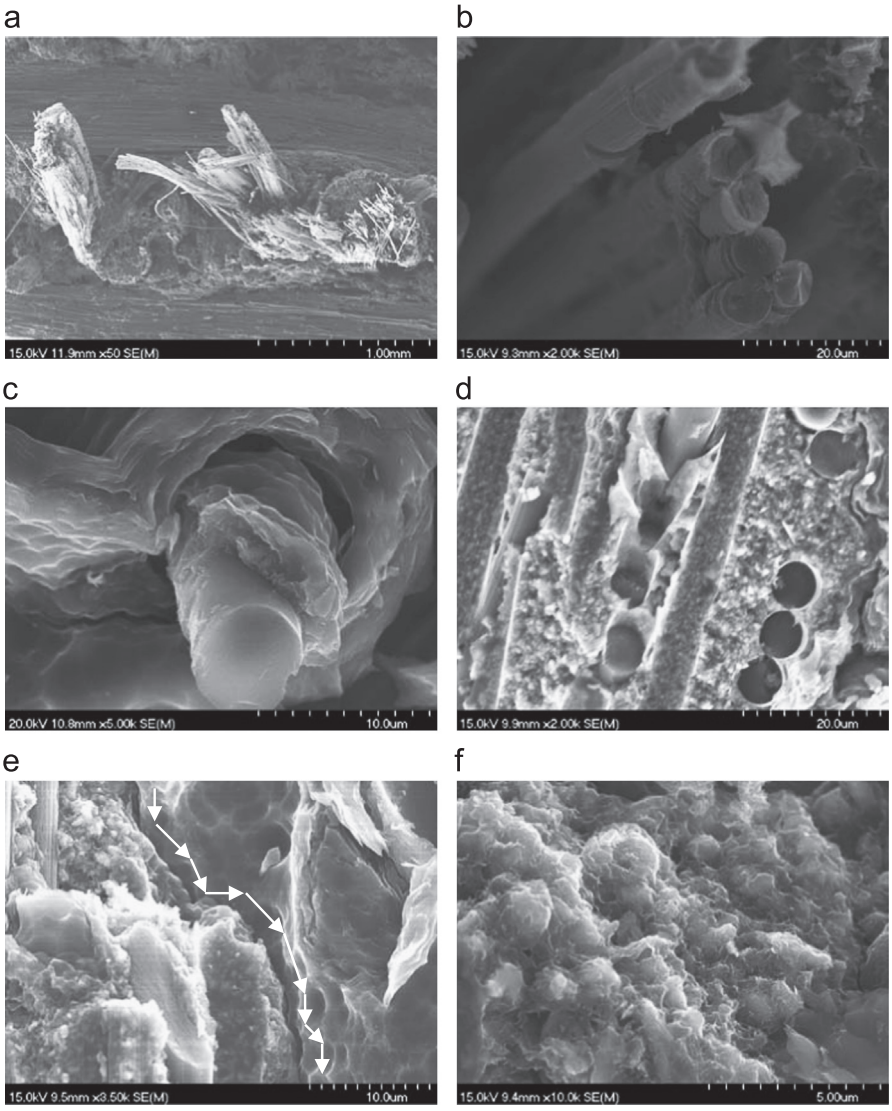

Fig. 9. Fracture profiles of C/C–SiC: (a) fracture surface whole morphology (top view); (b) filler pullout; (c) amplified photo of fiber pullout; (d) fiber/matrix interfaces after fiber pullout; (e) crack deflection within matrix; (f) magnified matrix fracture surface.

enwrapping, encircling and embedding were the main modes. For C/C–SiC, embedding was the main one. There were three kinds of characteristic fiber/matrix interfaces: (fiber/filler/PyC)$_n$/PyC, fiber/(filler/PyC)/PyC, fiber/filler/PyC.

(3) The flexure strength of C/C was 98 MPa, whereas those of C/C–B_4C and C/C–SiC were 200 and 140 MPa, respectively. The addition of ceramic filler not only increased the bonding strength of some fiber/matrix interface, but also toughened the PyC matrix.

Acknowledgments

The authors acknowledge the financial supports of Natural Science Foundation of China (No. NSFC50672076) and Doctoral Starting up Foundation of Xi'an University of Architecture and Technology in China (RC1039). The authors would like to give their special thanks to Prof. Dr. Yongdong Xu for his kind help on many aspects of scientific research and his continual support in the time of difficulties. The authors would also like to give their special thanks to Prof. Jihua Gou and Ricky McKee in University of Central Florida for their kind help in language correction.

References

[1] R. Gadow, M. Speicher, CMC brake disks in serial production-the competition between cost effectiveness and technical performance, Ceramic Engineering and Science Proceedings 23 (2002) 115–123.
[2] W. Krenkel, Microstructure tailoring of C/C–SiC composites, Ceramic Engineering and Science Proceedings 24 (4) (2003) 471–476.
[3] J.D. Chen, L.J.H. Chern, C.P. Ju, Effect of humidity on the tribological behavior of carbon–carbon composites [J], Wear 193 (1996) 38–47.
[4] S.-J. Park, M.-S. Cho, J.-R. Lee, P.-K. Pak, Influence of molybdenum disilicide filler on carbon–carbon composites, Carbon 37 (1999) 1685–1689.

[5] S.-J. Park, M.-S. Cho, Effect of anti-oxidative filler on the interfacial mechanical properties of carbon–carbon composites measured at high temperature, Carbon 38 (2000) 1053–1058.
[6] R. Gadow, A. Kienzle, Processing and manufacturing of C-fiber reinforced SiC-composites for disk brakes, in: K. Niihara (Eds.), in: Proceedings of the 6th International Symposium on Ceramic Materials and Components for Engines, Arita, Japan, 1997, pp. 412–418.
[7] R. Gadow, M. Speicher, Multilayer C/SiC composites for automotive brake systems, in: J.G. Heinrich, F. Aldinger (Eds.), Ceramic Materials and Components for Engines, Weinheim, Germany, 2001, pp. 565–570.
[8] A.G. Odeshi, H. Mucha, B. Wielage, Manufacture and characterisation of a low cost carbon fibre reinforced C/SiC dual matrix composite, Carbon 44 (2006) 1994–2001.
[9] H. Li, L. Zhang, L. Cheng, Y. Wang, Fabrication of 2D C/ZrC–SiC composite and its structural evolution under high-temperature treatment up to 1800 °C, Ceramics International 35 (2009) 2831–2836.
[10] X. Yin, S. He, L. Zhang, S. Fan, L. Cheng, G. Tian, T. Li, Materials Science and Engineering: A 527 (2010) 835–841.
[11] Y. Cai, S. Fan, H. Liu, L. Zhang, L. Cheng, J. Jiang, B. Dong, Mechanical properties of a 3D needled C/SiC composite with graphite filler, Materials Science and Engineering: A 527 (2010) 539–543.
[12] Y. Cai, Y. Xu, B. Li, S. Fan, L. Zhang, L. Cheng, L. Yu, Low-cost preparation and frictional behaviour of a three-dimensional needled carbon/silicon carbide composite, Journal of the European Ceramic Society 29 (2009) 497–503.
[13] M. Frieβ, W. Krenkel, R. Brandt, G. Neuer, Influence of process parameters on the thermophysical properties of C/C–SiC, in: W. Krenkel, R. Naslain, H. Schneider (Eds.), High Temperature Ceramic Matrix Composites, vol. 4, Weinheim: Wiley-VCH Press, 2001, pp. 328–333.
[14] S. Fan, L. Zhang, Y. Xu, L. Cheng, J. Lou, J. Zhang, Microstructure and properties of 3D needle-punched carbon/silicon carbide brake materials, Composites Science and Technology 67 (2007) 2390–2398.